



New miniature microstrip antenna for UWB wireless communications

Yaqeen S. Mezaal^{a*}, Kadhum Al-Majdi^b, Aqeel Al-Hilalli^a, Alabbas A. Al-Azzawi^a and
Aya A. Almkhtar^a

^a Medical Instrumentation Engineering Department, Al-Esraa University College, Baghdad, Iraq

^b Medical Instrumentation Engineering Department, Ashur University College, Baghdad, Iraq

Received 24 October 2021, accepted 4 January 2022, available online 17 May 2022

© 2022 Authors. This is an Open Access article distributed under the terms and conditions of the Creative Commons Attribution 4.0 International License CC BY 4.0 (<http://creativecommons.org/licenses/by/4.0>).

Abstract. A new miniature ultra-wideband (UWB) microstrip antenna was designed using a slotted patch resonator, and reduced ground plane realized on FR-4 substrate with 13×27.2 mm overall size. The designed antenna simulated by computer simulation technology (CST) electromagnetic simulator has three resonant frequencies of 3.1, 5.2, and 8.5 GHz with input reflection of -20.5 , -21.8 , and -22 dB for each resonance, respectively. The impedance bandwidth of 6.23 GHz is applicable for modern UWB wireless systems. The projected antenna has been fabricated and tested to corroborate the simulated S11 consequences, and the experimental consequences are in worthy compatibility with the simulated ones.

Keywords: UWB, microstrip antenna, slotted patch, reduced ground plane, compactness.

1. INTRODUCTION

The ultra-wideband (UWB) has become economically feasible for short-range, cost-effective communication owing to advances in high-speed microprocessors and quick switching techniques. Radar systems, wireless personal area networks, localization, consumer electronics, and medical electronics are just a few early applications. Since then, a complete grasp of UWB electromagnetics, components, and system engineering has been established. The Federal Communication Commission (FCC) of USA was the key organization to release UWB guidance in 2002, authorizing the unlicensed utilization of the allocated spectrum to be in the range of 3.1–10.6 GHz. Nevertheless, the allowed power level was set very low to escape the interference with the other technologies that function in this frequency range, such as Wi-Fi and Bluetooth [1]. Figure 1 depicts the usual radio transmission power spectral density against the

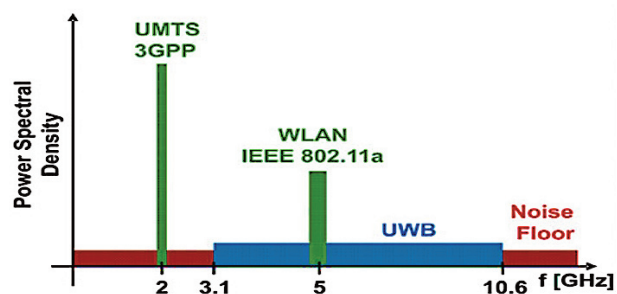


Fig. 1. Traditional radio signals power spectral density against the UWB signal.

UWB radio signal. Due to low transmission power, UWB systems are particularly susceptible to interference from neighboring narrowband systems [2].

An antenna system is a device that can send and receive data in a continuous loop. Therefore, the speed of the dispatch and receiving processes is critical to the rapid growth of countless communication technologies. Due to

* Corresponding author, yakeen_sbah@yahoo.com

the rapid growth in network users, fixed and mobile communication networks are requiring an expansion in the data rate for a wider frequency range. It is imperative that both mobile and wireless networks employ a larger bandwidth as a result of this. [3] The creation of antennas that are small, yet high-bandwidth and low-cost is consequently essential [4].

With its low power consumption, high data rate, excellent resistance to multipath propagation, and great reliability, UWB technology has emerged as a potential option for wireless communication systems. The high-frequency range can be utilized more to restrict microwave radiation using UWB-based techniques that operate in a wideband frequency spectrum. The microwave signal can pass through a variety of obstructions thanks to the low-frequency range's ability to penetrate [4].

Furthermore, before developing wide-speed and UWB-based antennas, it is necessary to evaluate the desired properties of the antennas under consideration. A thorough investigation of the numerous designs, analyses, and feeding methods applied in the fabrication of a microstrip antenna (MA) with better energy efficiency is required. Microwave configurations favor patch antennas because of their lightweight and low-cost construction, as well as their ability to be produced with high precision. Several studies in the literature have looked at ways to improve the patch antenna's performance and quality by tweaking its characteristics, such as input reflection, gain, path or total bandwidth [5,6].

Many other UWB-based antennas have been investigated and studied in the literature: widescreen microstrip, metamaterial, UWB wide-slot, broadband monopole, UWB taper slot antenna and dielectric resonator aerials antenna constituting a communications transceiver system. Transceivers are devices that receive data packets sent over the air. The efficiency of these antennas had to be enhanced in order to make robust transceivers. Additionally, the dielectric resonator (DR) is utilized in an antenna design known as the dielectric resonator antenna (DRA). A specific frequency can cause a dielectric material to produce a resonance peak. DRs are dielectric materials. It has been proven that these designs have a great Q-factor and can operate in a certain frequency range. The finishing antenna structure must contain a DR, a ground plane, and an excitation source to generate DR-based radiation [7].

Pentagonal-shaped UWB antennas are examined in [8]. UWB wearable technology, involving radio frequency identification (RFID), mobile devices, and wearable GPS, is expected to benefit from the antenna. Polyimide substrate with a thickness of 50 μm is used to construct the antenna. The bending impact has been examined according to the S parameter and radiation patterns. Before and after the bending, the pentagonal UWB antenna band-

width increased by 111.6 percent, going from 2.93 GHz to 10.3 GHz. Before and after bending, the antenna's gain is approximately 3 dB at 3.5 GHz, 5.2 GHz, and 5.8 GHz. Modern wearable equipment can make good use of this projected antenna.

An antenna that incorporates the WiBro (wireless broadband), WiMAX (worldwide interoperability for microwave access), ISM (Industrial, Scientific and Medical), and UWB services has been proposed in [9]. The rectangular monopole radiating element has two slots carved out of each corner. A third iteration Koch fractal curve has also been applied to the sidewalls of the radiator, except for the feed line direction. Feed lines are supported by a small rectangular hole in the ground. An offset 50 Ohm microstrip transmission line has been used to power the antenna. The feed line and antenna were printed on FR-4 (flame retardant woven glass-reinforced epoxy resin) substrates with a relative permittivity of 4.4 and a thickness of 1.59 mm. CST Microwave Studio was used to model and evaluate the proposed antenna's performance. According to the findings of the simulations, the proposed antenna has an impedance bandwidth of 2.3–11.5 GHz. In addition, the antenna radiating element proposed is 400 mm^2 in a compact size.

In [10], the researchers created a novel design for a compact MA used for the UWB applications feeds by using the stepped impedance line. The projected antenna has a rectangular shape for the patch with slots on its top face and a partially ground back with slots at its rear end to cover the criteria of the UWB technology. The designed antenna has a 34 \times 36 mm dimension, manufactured based on the FR-4 epoxy dielectric.

The design of a small UWB microstrip antenna is presented in [11]. The FR-4 substrate, which is 1.6 mm thick, is used to make the suggested antenna. The antenna is 28 \times 29 mm. Antennas with a hexagonal patch and a rectangular slot have a wider frequency response range. Additionally, the ground plane has been reduced and the antenna is being fed by a microstrip feeder. The antenna covers a bandwidth of 61.34 GHz, which is the equivalent of a 61.34 percent bandwidth. The highest gain is 6 dBi, with a return loss up to -40 dB.

UWB applications have sparked the interest of researchers looking for ways to make microstrip patch antennas smaller and lighter. The solution presented in [12] is an UWB monopole circular antenna with dual-band notch characteristics, which is further developed and modified. A split-ring circular slot and a mushroom electromagnetic bandgap structure are used to achieve the dual-band notch properties. Antenna is designed with a bandwidth of 2.0–12 GHz and a Voltage Standing Wave Ratio (VSWR) of 2 except in the WiMAX and WLAN bands of 3.2–3.7 GHz and 5.1–5.8 GHz, respectively.

WiMAX and upper WLAN interference are avoided by designing an octagonal antenna with dual band-

notched characteristics [13]. An octagonal patch antenna without notch filters was initially developed with a VSWR bandwidth of 9.06 GHz, operating in the UWB band (3.1–10.6 GHz). Complementary split ring resonator (CSRR) and the C-shaped slot have also provided dual-band rejection properties in this antenna's design.

It is shown in [14] that the band-notch characteristics are attained by utilizing a split ring slot (SRS) at WLAN frequency 5.3 GHz and satellite communication frequency 7.4 GHz using compact monopole antennas. Impedance matching in the frequency range of 3 to 12 GHz is achieved by modifying a rectangular patch. To generate WLAN band rejection, SRS is incorporated into the antenna geometry. The dimensions of this slot are adjusted to achieve the rejection at the X-band satellite frequency band.

In [15], the paper describes a small, wide-bandwidth spiral-shaped antenna (SSA) with dual alternative feeding methods (CPW-fed and microstrip lines). An SSA with both feed lines has a consistent radiation pattern, a wide impedance bandwidth, a constant group delay, and higher gain in the frequency ranges of 1.68 to 20 GHz and 1.23 to 20 GHz. There are also manufactured prototypes of projected SSAs that are tested and compared to simulated results.

The foremost goal of this paper is to design a new small ultra-wideband microstrip patch antenna. The design uses a single-layer substrate, slotted patch resonator, slotted microstrip feeder, and reduced ground plane to achieve these features. The projected antenna has UWB response and compactness to be employed in many wireless systems.

Section 2 of this paper describes in detail the configuration of a UWB antenna. Section 3 illustrates and discusses the projected antenna results in terms of S11 response, surface current intensity distribution, 3D radiation pattern, and far-field 2D radiation pattern. Section 4 depicts the fabrication process and compares simulated result with S11 measurement. As a final point, Section 5 provides the comprehensive conclusions of this study.

2. ANTENNA DESIGN

The microstrip antenna (MA) is comparatively considered as a modernistic concoction. It was created to deduct the available synthesis of an antenna and the other driving circuits used in the communication arrangement on a typical printed circuit board or the semiconductor flake. Aside from the other resulting benefits, the integrated-circuit technology for antenna manufacturing provided considerable dimensional precision, which was otherwise tricky to accomplish in standard fabrication processes. The structure of the MA usually contains a dielectric element named as 'substrate' of a specific thickness, having

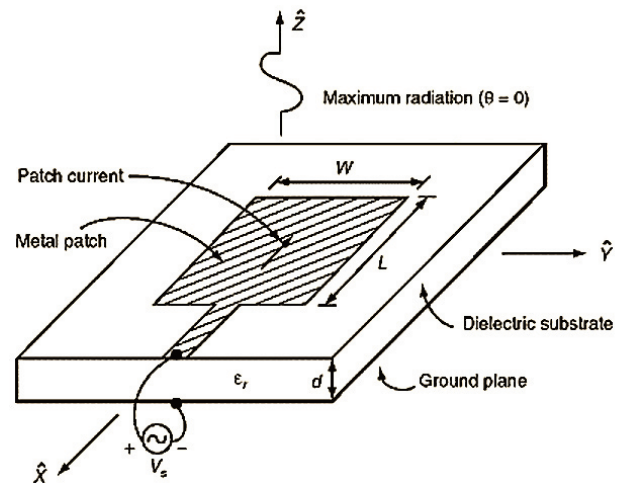


Fig. 2. Typical microstrip antenna.

an entire metallization on one of its outsides and of a metal 'patch' on the other surface. The substrate is ordinarily very fluffy. The used metal patch on the top surface could take a different appearance, though the rectangular configuration shown in Fig. 2 is practiced in general [16].

The MA is feasibly excited by employing multiple of the arrangements. One of the basic strategies is to feed the antenna using a microstrip line, combining the MA at a center of any edge. The microstrip line could be joined to the antenna feeder or straightforwardly fed by joining the signal source acrossed the microstrip line and the ground plane of an antenna [16].

It is known that slotted patch antennas have gained more attractiveness because of their UWB characteristics. These are very popular for wideband and volume-limited applications. Almost all the designs use the TM010 mode because it is the dominant mode of patch antenna in transverse magnetic.

The projected topology of the ultra-wideband antenna is illustrated in Fig. 3. This antenna is printed on an FR-4 substrate with relative permittivity of 4.3 and a thickness of 1.5 mm. The antenna feed is matched to 50 Ω.

The ground plane appears in a bottom layer with a length of 11.95 mm and width of 12 mm, and 0.035 mm ground thickness. Above the ground, there is a substrate. The substrate dimensions were 13 mm width and 27.2 mm length, while the substrate thickness was 1.5 mm. The dimensions of the projected antenna are depicted in Fig. 3.

The antenna's width and length based on the slotted patch radiator are calculated using the following equations [16]:

$$W = \frac{c}{2f_r} \sqrt{\frac{2}{\epsilon_r + 1}}, \quad (1)$$

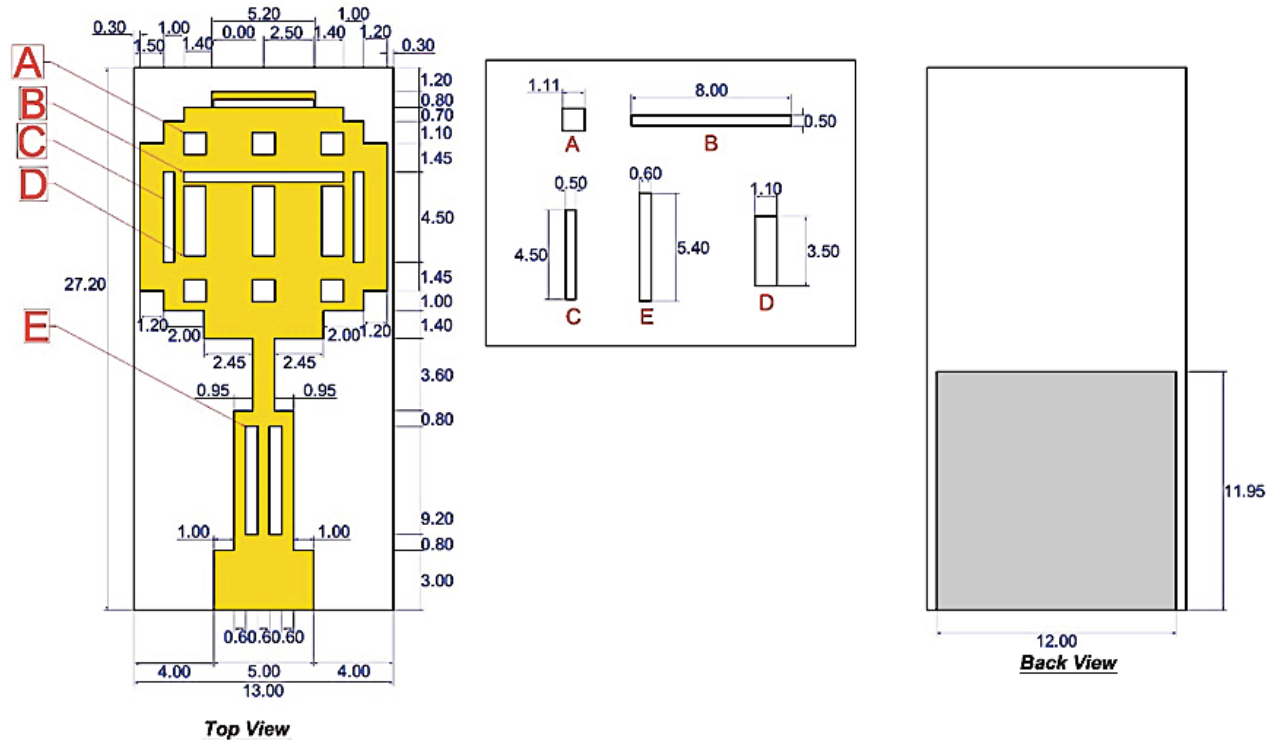


Fig. 3. The geometry for the projected antenna.

$$L = \frac{C}{2f_r \sqrt{\epsilon_{reff}}} - 2\Delta L, \quad (2)$$

C represents the velocity of light (0.3G m/s), f_r denotes resonance frequency, ϵ_r is a dielectric constant of FR-4 material, and ϵ_{reff} stands for the effective dielectric constant for the same material that was determined by CST simulator.

The equivalent circuit of the proposed antenna, based on L and C, is depicted in Fig. 4. L and C can be calculated based on reported equations in [17].

3. SIMULATION RESULTS AND DISCUSSION

The input reflection (S11) simulation for the projected antenna based on CST electromagnetic solver is shown in Fig. 5. At 3.1 GHz, an input reflection of -20.5 dB is achieved. At 5.2 GHz, an input reflection of -21.8 dB is achieved. At 8.5 GHz, an input reflection of -22 dB is achieved. The VSWR was 1.208 at 3.1 GHz, 1.177 at 5.2 GHz, and 1.173 at 8.5 GHz. Accordingly, the impedance bandwidth for the designed antenna is 6.23 GHz as depicted in Fig. 5.

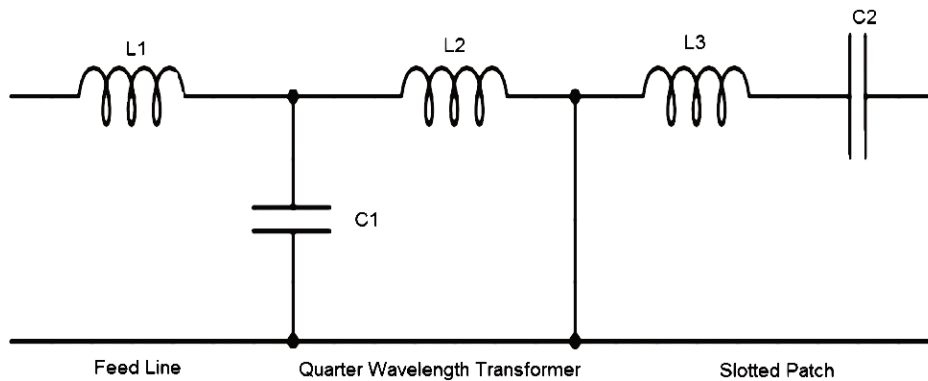


Fig. 4. The circuit equivalent of the projected antenna.

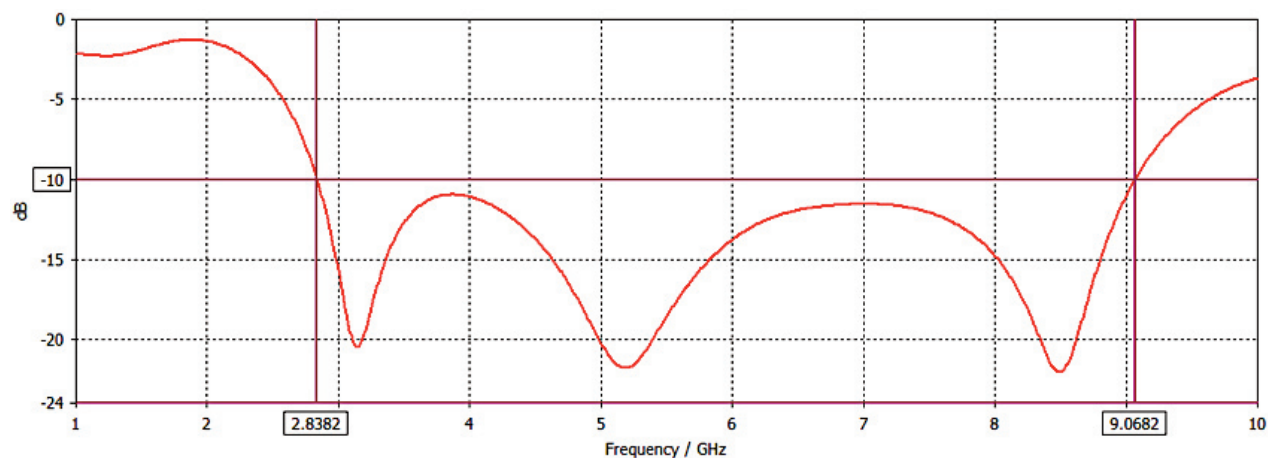


Fig. 5. Input reflection for the simulated antenna.

The radiation pattern in Fig. 6 indicates a three-dimensional depiction based on spherical coordinates (r , θ , Φ), supposing its starting point at the center of the spherical coordinate system. For this antenna, the gain is 1.36 dBi, as shown in Fig. 6.

Figure 7 shows the surface current distribution in the conductive portions of the proposed UWB antenna. The surface current distribution seen here is an actual electric current that has been induced by an external EM field. The feeder, the patch radiator bottom, and several edges of the decreased ground plane have distinct effective zones with a maximum magnetic strength of 118 A/m.

The IEEE gain for UWB antenna within effective impedance bandwidth is shown in Fig. 8. It ranges from 1.4 to 2.6 dBi within the 3–8 GHz frequency range. To further understand how far-distance patterns' radiation fields are represented in the xz , xy , and yz planes, see Fig. 9. Because the xy radiation patterns are perpendicular to the E-plane and coincide with the H-plane of a vertically polarized antenna, they are horizontal plane radiation patterns. The yz -plane and the E-plane have crossed paths. The yz patterns are a type of radiation pattern in the vertical plane.

The UWB antennas in this research article have been compared with reported antennas in [18–30]. The projected

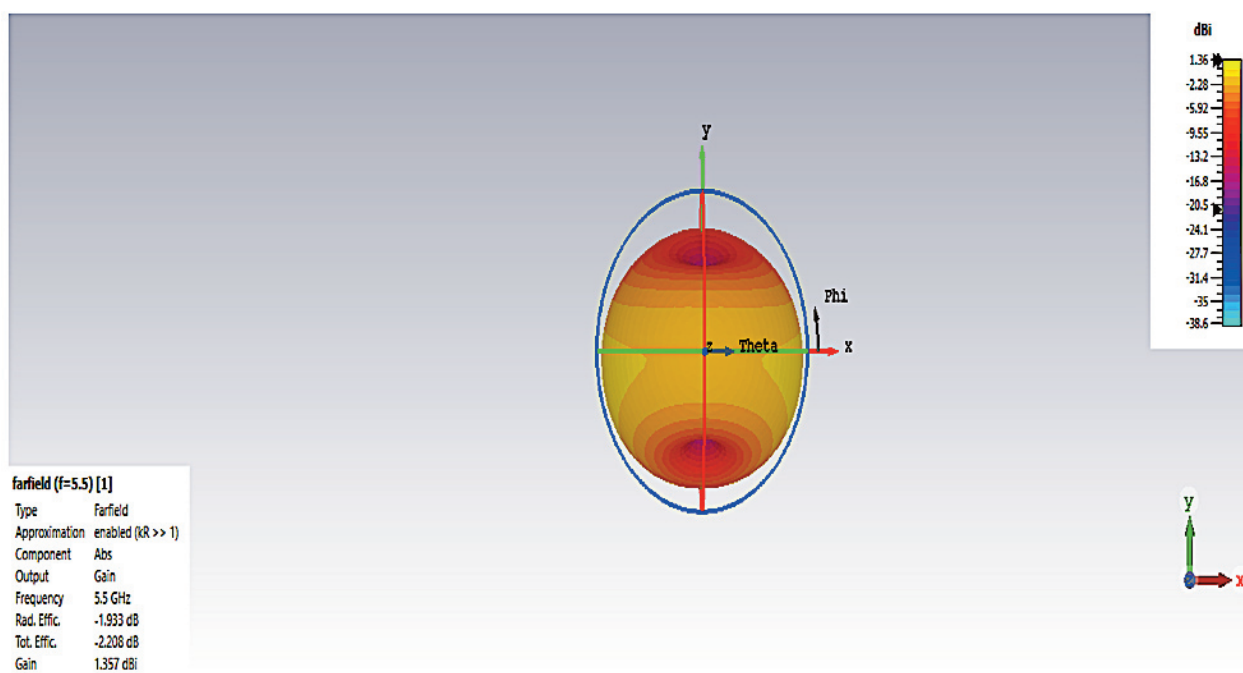


Fig. 6. 3D radiation patterns for the simulated antenna at 5.5 GHz.

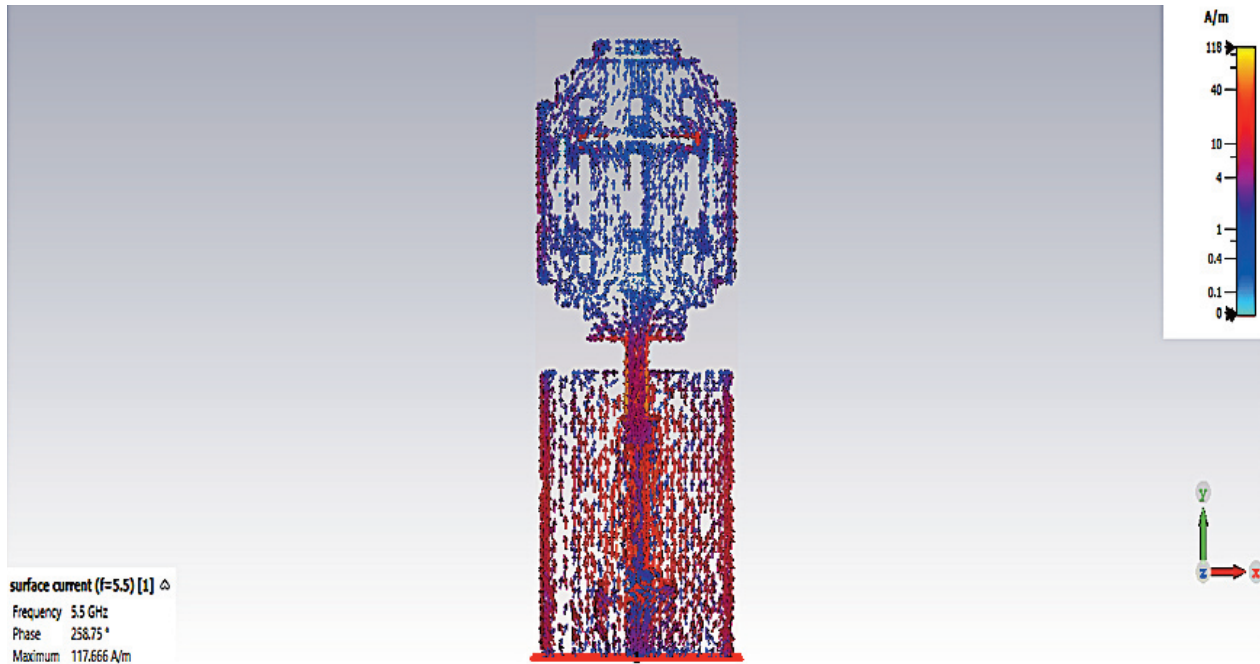


Fig. 7. Surface current intensity distribution for the simulated antenna at 5.5 GHz.

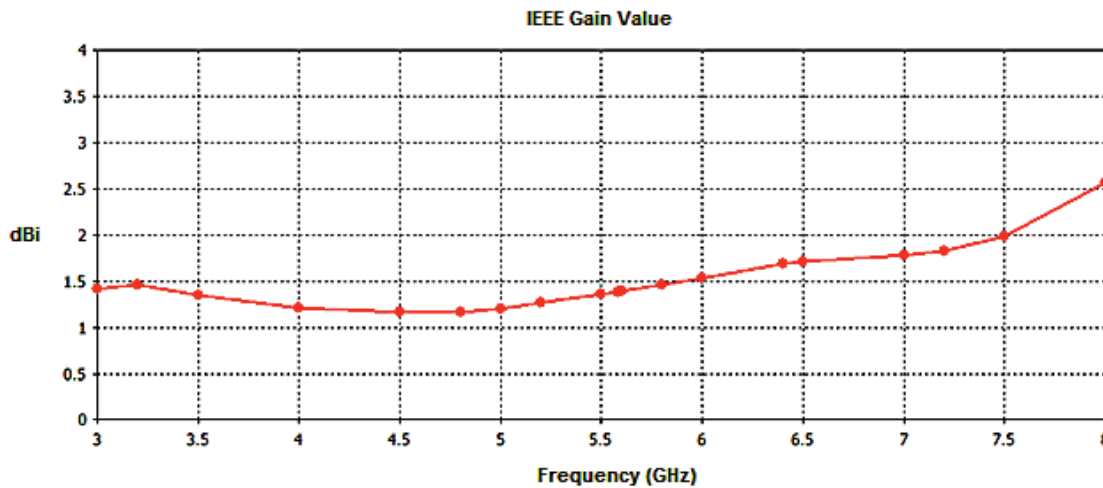


Fig. 8. Gain result for the projected antenna.

antenna in this study has the smallest size with competitive impedance bandwidth.

4. FABRICATION AND MEASUREMENTS

The projected UWB antenna was manufactured by means of LPKF machine, including design steps and optimization. A prototype was milled on the FR-4 epoxy substratum; as depicted in Fig. 10, an SMA coaxial con-

necter was connected to the antenna feed end. At that point, Anritsu 37369A Vector Network Analyzer was tested experimentally.

The measured and simulated antenna results are illustrated in Fig. 11. We can see that the measured and simulated effects are closely organized. Some inconsistencies can also exist between the simulation and the results of the measurement, especially the ripples in the measurement and impedance bandwidth. This is because of certain practical conditions such as SMA connector

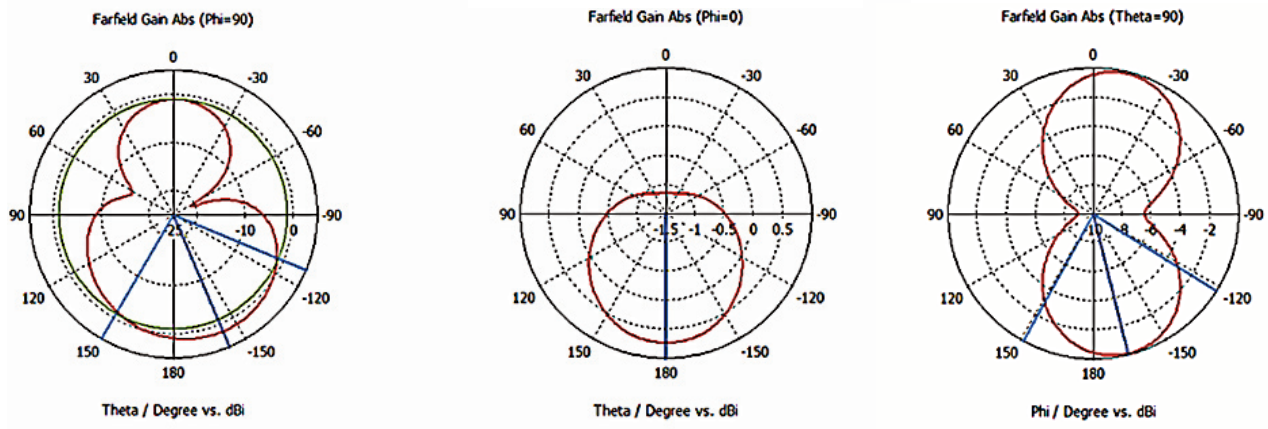


Fig. 9. Far-field radiation patterns for the projected antenna at 5.5 GHz.

Table 1. Comparison of the reported UWB antennas

Ref.	Dielectric constant	Size (mm ²)	Bandwidth range (GHz)
[18]	4.7	42 × 50	2.78–9.78
[19]	3.38	45 × 50	3–11.57
[20]	3.4	120 × 100	3–11
[21]	3.48	120 × 60	0.75–7.65
[22]	4.4	30 × 30	4–10
[23]	2.2	80 × 80	1.8–3.7 and 4.5–8.23
[24]	4.7	35 × 49	3.5–5.97
[25]	4.6	60 × 69	2–8
[26]	4.4	24 × 36	4.8–7.8
[27]	4.4	26.6 × 29.3	3.2–10.6
[28]	4.4	27 × 27	3.1–10.6
[29]	4.4	30 × 24	1.72–19.25
[30]	4.4	30 × 30	2.45–12.0
Proposed antenna	4.3	13 × 27.2	2.84–9.07

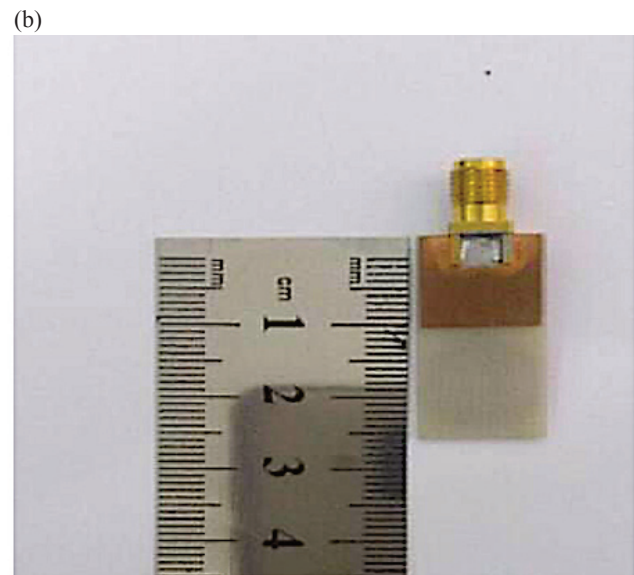
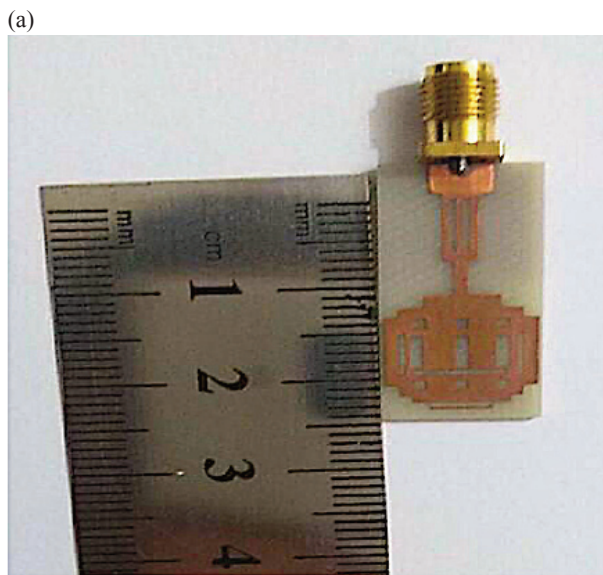


Fig. 10. The prototype of the designed UWB antenna: top view (a) and bottom view (b).

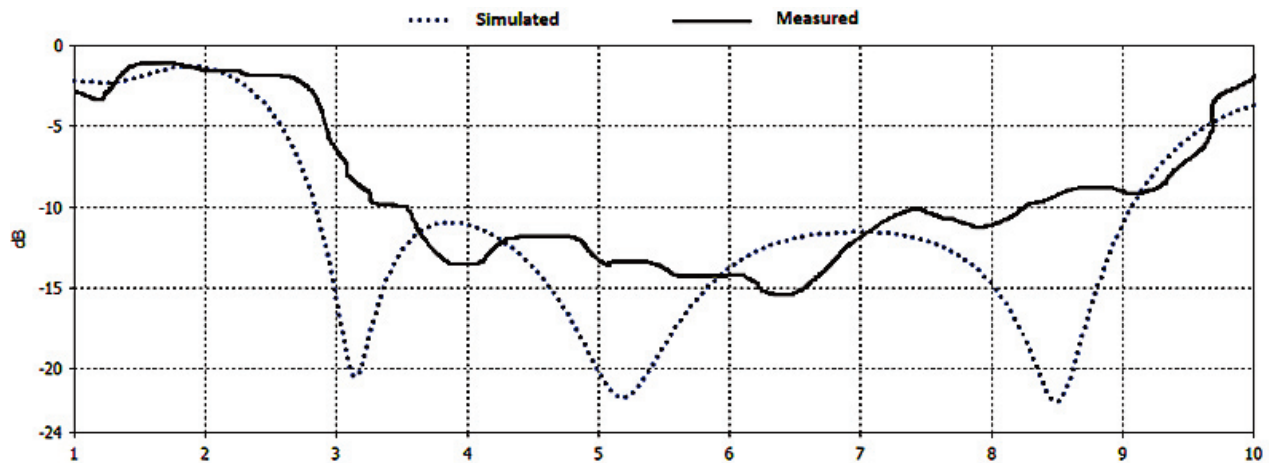


Fig. 11. The simulated and measured S11 consequences for the designed UWB antenna.

efficiency, potential noise in the lab environment, soldering effect, and manufacturing tolerance. The dielectric substrate constant has as well an unknown negative effect.

5. CONCLUSION AND FUTURE TREND

A miniaturized UWB antenna has been designed based on a slotted patch resonator, slotted feed and reduced ground plane. The designed antenna has a 13×27.2 mm overall size and it operates under the GHz frequency range of 2.84–9.07. It was created using (CST) Microwave Studio 3D EM simulation and analysis software. The antenna can be used in early diagnosis aids to detect early-stage breast tumors, which are seldom found, thus enabling quick and successful treatment. Breast tumor identification can be accomplished through various means, with mammography being the most widely employed. Mammography is a painful and limited X-ray procedure for detecting breast tumors. Microwave imaging that uses a microstrip antenna and microwave frequency to detect breast tumors, presents an appealing alternative to mammography.

ACKNOWLEDGEMENTS

The authors express their gratitude to Al-Esraa University College and Ashur University College in Iraq for supporting this study. The publication costs of this article were partially covered by the Estonian Academy of Sciences.

REFERENCES

1. Saeidi, T., Ismail, I., Wen, W. P., Alhawari, A. R. H. and Mohammadi, A. Ultra-wideband antennas for wireless communication applications. *Int. J. Antennas Propag.*, 2019, **2019**(4),1–25.
2. Tizyi, H., Riouch, F., Tribak, A., Najid, A. and Mediavilla Sanchez, A. CPW and microstrip line-fed compact fractal antenna for UWB-RFID applications. *Prog. Electromagn. Res. C*, 2016, **65**, 201–209.
3. Deal, W. R., Jung, T., Wu, M. C. and Itoh, T. All-optically controlled beam-scanning array for antenna remoting applications. *1998 IEEE MTT-S International Microwave Symposium Digest (Cat. No. 98CH36192), Baltimore, MD, USA, June 7–12, 1998*. IEEE, 1998, **3**, 1383–1386.
4. Antar, Y. M. M. Microstrip antenna design handbook [Book Review]. *IEEE Antennas Propag. Mag.*, 2003, **45**(2), 86.
5. Cicchetti, R., Faraone, A., Caratelli, D. and Simeoni, M. Wideband, multiband, tunable, and smart antenna systems for mobile and UWB wireless applications 2014. *Int. J. Antennas Propag.*, 2015, **2015**, 1–3.
6. Galvan-Tejada, G. M., Peyrot-Solis, M. A. and Jardon Aguilar, H. *Ultra Wideband Antennas: Design, Methodologies, and Performance*. CRC Press, London, 2017.
7. Dash, S. K. K., Khan, T. and Antar, Y. M. M. A state-of-art review on performance improvement of dielectric resonator antennas. *Int. J. Rf. Microw. C. E.*, 2018, **28**(6), 21–27.
8. Hammoodi, A. I. and Jawad K. A. Practical Bending studying on UWB pentagonal flexible antenna. In *Proceedings of 2020 IEEE International Symposium on Antennas and Propagation and North American Radio Science Meeting, Montréal, Canada, July 5–10, 2020*. IEEE, 2020, 413–414.
9. Yassen, M. T., Ali, J. K., Salim, A. J., Abdulkareem, S. F., Ali I. Hammoodi, A.I. and Hussan, M. R. A Compact fractal based printed monopole antenna for WiBro, WiMax and UWB applications. *Int. J. Eng. Advanced Technol.*, 2013, **3**(1), 347–351.

10. Mazhar, W., Tarar, M. A., Tahir, F. A., Ullah, S. and Bhatti, F. A. Compact microstrip patch antenna for ultra-wideband applications. In *PIERS Proceedings, Stockholm, Sweden, August 12–15, 2013*. The Electromagnetics Academy, 2013, 1100–1104.
11. George, N. and Lethakumary, B. A compact microstrip antenna for UWB applications. *Microw. Opt. Technol. Lett.*, 2015, **57**(3), 621–624.
12. Bhatia, S. S., Sivia, J. S., Sharma, N. and Sharma, V. Electromagnetic bandgap structure and split ring slot-based monopole antenna for ultra-wideband applications with dual-band notch characteristics. *Eng. Rep.*, 2020, **2**(10), e12239.
13. Sharma, N., Bhatia, S. S., Sharma, V. and Sivia, J. S. An octagonal shaped monopole antenna for UWB applications with band notch characteristics. *Wirel. Pers. Commun.*, 2020, **111**(3), 1977–1997.
14. Kaur, K., Kumar, A. and Sharma, N. Split ring slot loaded compact CPW-fed printed monopole antennas for ultra-wideband applications with band notch characteristics. *Prog. Electromagn. Res. C*, 2021, **110**, 39–54.
15. Sharma, N. and Bhatia, S. S. Design printed UWB antenna with CPW and microstrip-line-fed for DCS/PCS/Bluetooth/WLAN wireless applications. *Int. J. Rf. Microw. C. E.*, 2021, **31**(1), e22488.
16. Balanis, C. A. *Antenna theory: Analysis and Design*. 4th ed. John Wiley & Sons, Hoboken, 2016.
17. Sharma, N. and Sharma, V. A design of microstrip patch antenna using the hybrid fractal slot for wideband applications. *Ain Shams Eng. J.*, 2018, **9**(4), 2491–2497.
18. Liang, J., Chiau, C. C., Chen, X. and Parini, C. G. Study of a printed circular disc monopole antenna for UWB systems. *IEEE Trans. Antennas Propag.*, 2005, **53**, 3500–3504.
19. Yassin, M. E., Mohamed, H. A., Abdallah, E. A. F. and EI-Hennawy, H. S. Circularly polarized wideband-to narrowband switchable antenna. *IEEE Access*, 2019, **7**, 36010–36018.
20. Sadat, S., Fardis, M., Geran, F., Dadashzadeh, G., Hojjat, N. and Roshandel, M. A compact microstrip square-ring slot antenna for UWB applications. In *Proceedings of the 2006 IEEE Antennas and Propagation Society International Symposium, Albuquerque, NM, USA, July 9–14, 2006*. IEEE 4629–4632.
21. Gopikrishna, M., Krishna, D. D., Aanandan, C. K., Mohanan, P. and Vasudevan, K. Compact linear tapered slot antenna for UWB applications. *Electron. Lett.*, 2008, **44**, 1174–1175.
22. Hussain, R., Sharawi, M. S. and Shamim, A. An integrated four-element slot-based MIMO and a UWB sensing antenna system for CR platforms. *IEEE Trans. Antennas Propag.*, 2018, **66**, 978–983.
23. Low, Z. N., Cheong, J. H. and Law, C. L. Low-cost PCB antenna for UWB applications. *IEEE Antennas Wirel. Propag. Lett.*, 2005, **4**, 237–239.
24. Lim, M. C., Rahim, S. K. A., Hamid, M. R., Eteng, A. A. and Jamlos, M. F. Frequency reconfigurable antenna for WLAN application. *Microw. Opt. Technol. Lett.*, 2017, **59**(1), 171–176.
25. Dahalan, F. D., Rahim, S. K. A., Hamid, M. R., Rahman, M. A., Nor, M. Z. M. et al. Frequency-reconfigurable archimedean spiral antenna. *IEEE Antennas Wirel. Propag. Lett.*, 2013, **12**, 1504–1507.
26. Bhanumathi, V. and Swathi, S. Bandwidth enhanced microstrip patch antenna for UWB applications. *ICTACT J. Microelectronics*, 2019, **4**(4), 669–675.
27. Vijayalakshmi, J. and Murugesan, G. A miniaturized high-gain (MHG) ultra-wideband unidirectional monopole antenna for UWB applications. *J. Circuits, Syst. Comput.* 2019, **28**(13), 1950230.
28. Kaur, K., Kumar, A. and Sharma, N. Sprocket gear wheel-shaped printed monopole ultra-wideband antenna with band notch characteristics: Design and measurement. *Int. J. Rf. Microw. C. E.*, 2022, **32**(3). <https://doi.org/10.1002/mmce.22989>
29. Sharma, N. and Bhatia, S. S. Ultra-wideband fractal antenna using rhombus shaped patch with stub loaded defected ground plane: Design and measurement. *Int. J. Electron. Commun.*, 2021, **131**.
30. Sharma, N. and Bhatia, S. S. Design of printed monopole antenna with band notch characteristics for ultra-wideband applications. *Int. J. Rf. Microw. C. E.*, 2019, **29**(10). <https://doi.org/10.1002/mmce.21894>.